Trop J Nat Prod Res, January 2025; 9(1): 378 - 389 ISSN 2616-0684 (Print)
ISSN 2616-0692 (Electronic)

Tropical Journal of Natural Product Research

Available online at https://www.tjnpr.org

Original Research Article

Molecular Modelling Studies of Anti-Photoaging Activity of Patchouli (*Pogostemon cablin* Benth.) Essential Oil

Haya Maghfira[1], Essy Harnelly[2,5]*, Didik H. Utomo[3], Zulkarnain[4,5]

[1]*Master Program in Biology Department, Faculty of Mathematics and Natural Sciences, Syiah Kuala University, Banda Aceh 23111, Aceh, Indonesia*
[2]*Departement of Biology, Faculty of Mathematics and Natural Sciences, Syiah Kuala University, Banda Aceh 23111, Aceh, Indonesia*
[3]*Bioinformatics Research Center, Institute of Bioinformatics Indonesia, Malang 65162, East Java, Indonesia*
[4]*Department of Biomedical Science, Faculty of Medicine, Syiah Kuala University, Banda Aceh 23111, Aceh, Indonesia*
[5]*ARC-PUIPT Nilam Aceh, Syiah Kuala University, St. Tgk. Syech Abdul Rauf, Banda Aceh 23111, Indonesia.*

ARTICLE INFO

Article history:
Received 29 August 2024
Revised 06 September 2024
Accepted 06 December 2024
Published online 01 February 2025

ABSTRACT

Skin aging is a natural process of change in all living organisms, it is associated with cell maturation. Cells gradually lose function on exposure to factors such as sunlight, pollution, or prolonged contact with chemicals. Patchouli Essential Oil (PEO) extracted from Patchouli Plant (*Pogostemon cablin* Benth.) is known to have antioxidants and anti-aging properties. Therefore, this study aimed to determine the potential of PEO as an anti-aging agent using *in silico* methods. PEO Chemical Profiling was done using Gas Chromatography-Mass Spectrometry (GC-MS). Each PEO active molecule was subjected to ADME (Adsorption, Distribution, Metabolism, and Excretion) analysis using Lipinski's Rule of Five and LogKp (Skin Permeability) in the SwissADME database, followed by toxicity test using the ProTox-II database. Each of the selected compounds was subjected to reverse docking against skin-aging proteins known to play important roles in the aging process including MMP13 (Collagenase), MMP9 (Gelatinase), and hyaluronidase using the Autodock Vina program integrated into the PyRx software. In addition, Molecular Dynamics Simulation (MDS) was carried out using YASARA (Yet Another Scientific Artificial Reality Application) v.23.5.19 software. GC-MS analysis of PEO detected 44 compounds, out of which 26 compounds with anti-aging potential were selected based on ADME and toxicity studies. Molecular docking result showed that the compound 3, 7, 11-trimethyl-dodeca-2, 4, 6, 10-tetraenal had the lowest binding energy value (-8.2 Kcal/mol) against the MMP9 protein. MDS data also demonstrated excellent interaction between ligand molecule and MMP9 protein. These results imply that PEO compounds may inhibit the function of skin-aging proteins.

Keywords: Skin Aging, Molecular Modelling, Patchouli Essential Oil, Active compounds, ADME analysis.

Introduction

Natural products are renowned for playing a central role in the treatment and prevention of human diseases. According to the World Health Organization (WHO), about 75% of the global population still rely on plant-based traditional medicine to maintain their health.[1] Natural products are a major source of compounds used in the discovery and development of traditional medicines. Nature has been the source of beneficial biological agents, and a large number of pharmaceuticals have recently been generated from natural sources based on their traditional medicinal value.[2]Essential oils are a popular natural product derived from plant parts such as roots, stems, leaves, flowers, and even fruits. Patchouli (*Pogostemon cablin*) is a plant that produces essential oil, which is extracted by steam distillation from dried leaves.[3] Essential oils provide benefits such as antioxidant activity, which are necessary for health maintenance. Antioxidants are frequently used in cosmetic products due to their ability to combat issues related to skin aging.

*Corresponding author. E mail: essy.harnelly@usk.ac.id

Tel: +62 812-6213-1992

Citation: Maghfira H, Harnelly E, Utomo DH, Zulkarnain. Molecular Modelling Studies of Anti-Photoaging Activity of Patchouli (*Pogostemon cablin* Benth.) Essential Oil.Trop J Nat Prod Res. 2025; 9(1): 378 - 389
https://doi.org/10.26538/tjnpr/v9i1.48

Official Journal of Natural Product Research Group, Faculty of Pharmacy, University of Benin, Benin City, Nigeria

Cosmetic products also contain other chemical components found in essential oils, such as idebenone, arbutin, kinetin, tocopherol (vitamin E), ubiquinone, lipoic acid, polyphenols, flavonoids, and carotenoids, which are useful in addressing skin problems.[4]The aging process is a natural transformation that appears in all living beings, defined by changes in physical, psychological, and social situations. It is also related to the process of cell maturation, where cells grow and develop until reduction in function occurs, and this is usually induced by several factors, including environmental factors such as exposure to heat, sunlight, and lifestyle.[5] One of the major causes of skin aging is exposure to sunlight radiation, which promotes photoaging. This phenomenon occurs when proteins such as collagenase, gelatinase, elastase, hyaluronidase, and tyrosinase are activated, causing damage to the extracellular matrix of the skin. Natural ingredients in anti-aging products can suppress the action of these proteins when the skin is exposed to sunlight.[6] Generally, photoaging stimulates the production of radicals known as free radicals or reactive oxygen species (ROS), which promotes the proliferation of cells and activates certain proteins in the skin, which leads to alteration in the structure of the skin.

ROS are presumably molecules responsible for changes to the extracellular matrix of the skin during intrinsic photoaging.[7] In general, ROS activates downstream signalling pathways, including AP-1, NF-κB, and MAPK. Photoaging reduces collagen synthesis by activating NF-κB and AP-1, which enhance MMP gene transcription. AP-1 activation also causes increase in matrix metalloproteinases (MMPs), including MMP1 (collagenase) and MMP9 (gelatinase), as well as hyaluronidase levels. Wrinkles and sagging are indicators of premature

aging caused by the skin increased production of enzymes that degrade matrix tissue.[8]
Previous studies have investigated the inhibitory action of plant-derived chemicals on proteins that promote photoaging.[7-9] Furthermore, chemical compounds derived from animals, such as abalone shells (*Haliotis*), are used in addition to plant-derived chemicals.[12] Sinha *et al*.[13] conducted a study on the utilization of essential oils as anti-aging agents, but only the antioxidant properties were assessed. Some other studies on the anti-aging action of essential oils have also focused primarily on the antioxidants. Therefore, additional investigations on other elements of the essential oil are required. *In silico* evaluation can be used to study natural chemicals. In this method, chemicals are initially examined for interactions with the target protein. Subsequently, a simulation screening is performed to determine whether the natural compounds have the potential for use as drugs, which spurs further studies, such as *in vitro* and *in vivo* investigations.[14]

Materials and Methods

PEO Chemical Profiling Using Gas Chromatography-Mass Spectrometry (GC-MS)
PEO was obtained from Atsiri Research Centre (ARC-PUI PT), Syiah Kuala University, Banda Aceh, Indonesia. Gas Chromatography-Mass Spectrometry (GC-MS) analysis of the PEO was conducted using a Shimadzu GC-2010 plus a gas chromatograph. The mixture was separated using a TG-5MS capillary column measuring 30 m in length with an inner diameter of 0.2 mm and film thickness of 0.25 µm. About 1 microlitre of the PEO was injected in a split mode (split ratio 1:10) into the GC apparatus. The temperature program included heating from 60°C to 150°C for 4 h, and then to 250°C. Helium was used as the carrier gas at a flow rate of 1.35 mL/min, and ionization of the sample was achieved in a post-column electron impact ion source at 70 eV. The obtained peaks were compared with the mass spectrum database based on NIST (NIST, Gaithersburg, MD, USA) using Chromeleon software.

Screening the Active Compounds of PEO
The GC-MS analysis showed 44 active chemical components in PEO.[15] The NIST Chemistry Webbook (https://webbook.nist.gov/chemistry/) was used to verify all PEO components and the IUPAC Standard InChIKey information for each chemical was collected. InChIKey was used as a keyword to find molecules in the PubChem database (https://pubchem.ncbi.nlm.nih.gov). The structure, SMILES, Chemical ID (CID), and chemical formula were downloaded and gathered. Compounds without 3D structures and sharing the same identity were removed.

ADME analysis and Toxicity test of PEO Compounds
Each PEO active molecule was assessed for ADME (Adsorption, Distribution, Metabolism, and Excretion) properties using Lipinski's Rule of Five and LogKp (Skin Permeability). The study was performed by submitting canonical SMILES list of each compound into the SwissADME database (http://www.swissadme.ch/). The compounds selected for the molecular docking process were those that did not violate any of Lipinski's rule of five requirements and fell within the expected LogKp range. However, before molecular docking, the selected compounds were examined for toxicity to predict mutagenecity, carcinogenecity, immunotoxicity, or cytotoxicity. The toxicity test was carried out using the ProTox-II database (https://tox-new.charite.de/protox_II/).

Collection and Preparation of Target Proteins
MMP13 (Collagenase, PDB ID 2D1N), MMP9 (Gelatinase, PDB ID 1GKC), and Hyaluronidase (PDB ID 1FCV) were the target protein structures used in this study. The 3D structure of each protein was obtained from the RCSB PDB database website (https://www.rcsb.org/). Each structure was created using the BIOVIA discovery studio tool, which eliminated H_2O molecules and native ligands previously attached to the protein.

Molecular Docking of Ligand and Protein
The molecular docking was carried out with the Autodock Vina program integrated into the PyRx software. The process was performed on the target protein active site. The grid box coordinates (x,y,z) for each protein were as follows: -22.46 Å, 38.82 Å, and -21.66 Å for MMP13, 40.16 Å, 14.89 Å, and 141.71 Å for MMP9, as well as -19.26 Å, 27.64 Å, and 16.61 Å for Hyaluronidase. Molecularly docked protein-ligand complexes were studied and visualized with the BIOVIA discovery studio. The binding site was assessed using ligand-residue interaction and 3D structure. After calculation, the docking score with the lowest binding energy value to the target protein was selected.

Molecular Dynamics Simulation
Molecular Dynamic Simulation was carried out using YASARA (Yet Another Scientific Artificial Reality Application) v.23.5.19 software. The parameters used included temperature 310K, NaCl ion 0.9, pH 7, and program running time 20000 ps (20 ns) in the md_run macro file. The program was run and completed, then data from molecular dynamic simulation were visualized in the form of graphical data created using GraphPad Prism 8.

Results and Discussion

PEO Active Compounds
The results of the GC-MS analysis of PEO showed that the active compounds present in PEO are mainly sesquiterpenes, with Patchouli alcohol as the major compound. Patchouli alcohol is a tricyclic sesquiterpene commonly used in the production of cosmetics, perfumes, and soaps.[16,17] The GC chromatogram of PEO is presented in Figure 1. From the chromatogram, the three most prominent peaks with percentage peak areas of 17.11% (7), 20.94%, (13), and 20.88% (24) with respective retention times of 21.53, 23.22, and 26.86, were identified as α-Guaiene, Azulene, 1,2,3,5,6,7,8,8a-octahydro-1,4dimethyl-7-(1-methylethenyl)-, [1S(1a,7a,8aß)]- (Gamma gurjunene), and Patchouli Alcohol, respectively. A comprehensive list of all the compounds detected are summarized in Table 1. Azulene, 1,2,3,5,6,7,8,8a-octahydro-1,4dimethyl-7-(1-methylethenyl)-, [1S(1a,7a,8aß)]- or Gamma gurjunene is known to have anti-inflammatory, and antioxidant properties. This compound also has calming and soothing properties leading to it frequent inclusion in products designed for sensitive skin to alleviate discomfort and irritation.[18] Patchouli alcohol reportedly possesses anti-inflammatory, antiulcerogenic, antibacterial, and antifungal properties.[4] Meanwhile, α-Guaiene has antimicrobial and anti-inflammatory activity. This compound is also used as an aromatic agent because it contributes to the distinctive aroma of Patchouli oil, widely used in perfumes and aromatherapy for calming effects.[19]
Several studies have shown that PEO compounds have pharmaceutical benefits.[11,20-22] However, the specific compound playing specific role is unknown. In this study, PEO compounds as well as reference compounds (Niacinamide, Retinol, and Hyaluronic acid) were obtained from the PubChem database.[23] A total of forty-four (44) compounds were selected based on the availability of information in the database (Table 1).

ADME Analysis and Toxicity Test Result of PEO Active Compounds
The SwissADME database was used to conduct ADME analyses on PEO active compounds. ADME analysis was used to evaluate the physicochemical properties, including drug-likeness, lipophilicity, solubility, flexibility, and other criteria.[24] Compounds obtained from natural sources cannot all be considered as drug candidates. Therefore, the primary goal of ADME analysis is to identify candidates with high biological activity and low toxicity, making it easy to select the appropriate compounds.
The ADME analysis performed in this study include the Lipinski's rule of five, which state that a compound to be used as drug must have the following characteristics; (1) a molecular weight of less than 500 Da, (2) a log P value of less than 5 (≤4.15), (3) hydrogen bond donors less than 5, and (4) hydrogen bond acceptors less than 10. Compounds that meet these conditions are selected as drug candidates.[25]

Table 1: Active compounds (ligands) of *Pogostemon cablin* Benth. PEO and reference compounds

No	Compound Name	Chemical ID	Reference
1	2-Pentene, 4,4-dimethyl-	5326158	This Study
2	Cyclohexene	89316	This Study
3	4,7-Methanoazulene	129829942	This Study
4	Caryophyllene	5281515	This Study
5	alpha-guide	5317844	This Study
6	Gamma-gurjunene	90805	This Study
7	Aciphyllene	565709	This Study
8	Alpha-Maaliene	102361380	This Study
9	Nootkatene	74427712	This Study
10	Caryophyllene oxide	1742210	This Study
11	Beta-Acorenol	6430766	This Study
12	Patchouli Alcohol	10955174	This Study
13	Cis-Z-a-Bisabolene epoxide	91753574	This Study
14	Naphthalenone	612605	This Study
15	Shyobunol	520758	This Study
16	3-Hexen-1-ol, 2,5-dimethyl-, acetate, (Z)-	5363388	This Study
17	(3aS,8aS)-6,8a-Dimethyl-3-(propan-2-ylidene)1,2,3,3a,4,5,8,8a-octahydroazulene	641722	This Study
18	Naphthalene	21587613	This Study
19	1,1,4,7-Tetramethyl-1a,2,3,4,6,7,7a,7b-octahydro-1Hcyclopropa[e]azulene	89532	This Study
20	(2S,4aR,8aR)-4a,8-Dimethyl-2-(prop-1-en-2-yl)1,2,3,4,4a,5,6,8a-octahydronaphthalene	10123	This Study
21	(1S,7S,8aR)-1,8a-Dimethyl-7-(prop-1-en-2-yl)-1,2,3,7,8,8ahexahydronaphthalene	91710361	This Study
22	Boronal	5369997	This Study
23	Humulenol-II	102115341	This Study
24	1H-Cycloprop[e]azulen-7-ol, decahydro-1,1,7-trimethyl-4methylene-,	91747864	This Study
25	(-)-Globulol	12304985	This Study

26	1,4-Dimethyl-7-(prop-1-en-2-yl) decahydroazulen-4-ol	5320651	This Study
27	Acetic acid, 3-Hydroxy-6-isopropenyl	540542	This Study
28	3,7,11-Trimethyl-dodeca-2,4,6,10-tetraenal	5365928	This Study
29	2,2-Dimethyl-4-octenal	5367755	This Study
30	(1S,2E,6E,10R)-3,7,11,11Tetramethylbicyclo [8.1.0] undeca-2,6diene	13894533	This Study
31	Valerena-4,7(11)-diene	58067884	This Study
32	Bicyclo[5.3.0]decane, 2-methylene-5-(1methylvinyl)-8-methyl-	564533	This Study
33	2-Isopropenyl-4a,8-dimethyl1,2,3,4,4a,5,6,8a-octahydronaphthalene	605019	This Study
34	Selina-3,7(11)-diene	522296	This Study
35	(+)-Isovalencenol	5352472	This Study
36	2,3,3-Trimethyl-2-(3-methyl-buta-1,3dienyl)-cyclohexanone	5371301	This Study
37	Longipinocarveol, trans-	534645	This Study
38	Humulene epoxide I	5463721	This Study
39	2-(4a,8-Dimethyl-1,2,3,4,4a,5,6,7octahydro-naphthalen-2-yl)-prop-2-en-1-ol	579791	This Study
40	Ledol	92812	This Study
41	8aH-2,4a-methanonaphthalen-8a-ol, octahydro-1,1,5,5-tetramethyl-	534931	This Study
42	2,3,3-Trimethyl-2-(3-methylbuta-1,3dienyl)-6-methylenecyclohexanone	5373835	This Study
43	Beta,7BetaH,10a-Eudesm-11-en-1a-ol	494439	This Study
44	6-Isopropenyl-4,8a-dimethyl1,2,3,5,6,7,8,8a-octahydronaphthalene2,3-diol	535221	This Study
45	Niacinamide (R1)	936	[22]
46	Retinol (R2)	445354	[22]
47	Hyaluronic acid (R3)	24759	[22]

Another measure is log Kp, which represents the permeation rate constant when the compound penetrates the skin depending on partitioning behaviour (skin pores) and molecular size. Log Kp quantifies the permeation rate of a substance as it travels through the stratum corneum of the skin, making the parameter useful for topical medication development.[26]

Screening using ADME analysis showed that 26 out of 44 PEO compounds had the potential to be used as anti-aging skin drug candidates (Table 2). The 26 compounds follow Lipinski's rule of five and fall within the expected log Kp range (-6.11 cm/s to -0.19 cm/s).[27] The remaining 18 compounds did not meet all Lipinski's requirements, for example, their log P values were greater than 5 (≤4.15), but still fell within the expected log Kp range.

Table 2: ADME analysis result based on Lipinski's rule of five and LogKp (Skin permeability)

Compound	Lipinski's Rule of Five				LogKp (Skin Permeability)
	MW≤ 500	MLOGP ≤ 4.15	N or O ≤ 10	NH or OH ≤ 5	
PEOC1	98.19 g/mol	3.72	0	0	-4.78 cm/s
PEOC10	220.35 g/mol	3.67	1	0	-5.12 cm/s
PEOC11	222.37 g/mol	3.67	1	1	-4.92 cm/s
PEOC12	222.37 g/mol	3.81	1	1	-4.78 cm/s
PEOC13	220.35 g/mol	3.56	1	0	-4.94 cm/s
PEOC14	218.33 g/mol	3.46	1	0	-5.35 cm/s
PEOC15	222.37 g/mol	3.56	1	1	-4.23 cm/s
PEOC16	142.20 g/mol	1.85	2	0	-5.83 cm/s
PEOC22	206.32 g/mol	3.21	0	0	-5.17 cm/s
PEOC23	220.35 g/mol	3.46	1	1	-5.17 cm/s
PEOC24	220.35 g/mol	3.67	1	1	-5.44 cm/s
PEOC25	222.37 g/mol	3.81	1	1	-5.00 cm/s
PEOC26	222.37 g/mol	3.67	1	1	-4.59 cm/s
PEOC27	278.39 g/mol	2.96	3	1	-5.85 cm/s
PEOC28	218.33 g/mol	2.96	1	0	-5.85 cm/s
PEOC29	140.22 g/mol	2.28	1	0	-5.35 cm/s
PEOC35	220.35 g/mol	3.56	1	1	-5.35 cm/s
PEOC36	206.32 g/mol	3.21	1	0	-4.55 cm/s
PEOC37	220.35 g/mol	3.67	1	1	-4.91 cm/s
PEOC38	220.35 g/mol	3.67	1	0	-4.91 cm/s
PEOC39	220.35 g/mol	3.56	1	1	-5.05 cm/s
PEOC40	222.37 g/mol	3.81	1	1	-5.00 cm/s
PEOC41	222.37 g/mol	3.81	1	1	-4.81 cm/s
PEOC42	218.33 g/mol	3.37	1	0	-4.22 cm/s
PEOC43	222.37 g/mol	3.67	1	1	-4.43 cm/s
PEOC44	236.35 g/mol	2.63	2	2	-6.00 cm/s
RC1	122.12 g/mol	-0.43	2	1	**-7.31 cm/s**
RC2	286.45 g/mol	**4.48**	1	1	-4.01 cm/s
RC3	776.65 g/mol	-8.03	**23**	**14**	**-16.31 cm/s**

PEOC: Patchouli Essential Oil Compound;
The bolded value indicates the violation of Lipinski's rule of five and the expected logKp range value.

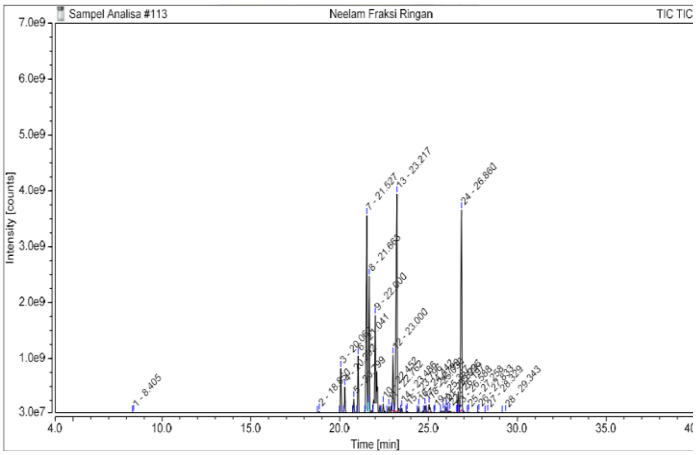

Figure 1: Gas chromatogram of the PEO with the major compounds detected

All three reference compounds (RC) used violated both the Lipinski rule and the expected log Kp. These three compounds are widely used in skincare products, but only on the outer skin. Based on ADME analysis results, PEO compounds have log Kp values within the predicted range, indicating optimal absorption through the skin.

Hyaluronic acid (HA) is a glycosaminoglycan (GAG) that contains negatively charged polysaccharide molecules. The molecule is made up of repeating glucuronic acid and N-acetyl glucosamine units. The negatively charged nature makes hyaluronic acid extremely hydrophilic and soluble in water.[28] These features make this compound suitable for use as a moisturizer to prevent dryness of the skin surface. Nicotinamide (NAM) and nicotinic acid (NA), also known as vitamin B3 (or niacin), are water-soluble vitamins of the B complex. Both NAM and NA are components of the cofactor enzymes nicotinamide adenine dinucleotide (NAD) and nicotinamide adenine dinucleotide phosphate (NADP), which serve important physiological functions in a variety of redox reactions. Hyaluronic acid coupled with niacinamide can limit the degradation process by hyaluronidase enzyme with longer extended activity compared to conventional HA, according to *in vivo* data.[29]

Toxicity studies were carried out on the 26 selected compounds to evaluate their carcinogenic, immunotoxic, mutagenic, or cytotoxic properties and the results are presented in Table 3. Most compounds were classified as toxicity classes 4 and 5, suggesting the potential to cause harm when consumed. However, these compounds are less hazardous compared to classes 1–3.[30] The LD_{50} (Lethal Dose) of each compound ranged from 940 to 5000 mg/kg, which is higher than that of the three control compounds (RC1, RC2, and RC3). This indicates that the PEO compound is less toxic than the three control compounds. Although these compounds are not poisonous, consumption should be in the appropriate dose. Toxic compounds, even when the probability is minimal, are excluded from the docking process.[30]

Molecular Docking Result

Molecular docking was used to demonstrate the interaction between the ligand and the target protein.[31] Each target protein, MMP13 (collagenase), MMP9 (gelatinase), and hyaluronidase, was subjected to molecular docking, and the results are presented in Table 4. Based on the molecular docking data, PEO compounds PEOC13 (Cis-Z-a-Bisabolene Epoxide), PEO14 (Naphthalene), PEOC27 (Acetic acid, 3-Hydroxy-6-isopropenyl), and PEOC28 (3, 7, 11-Trimethyl-dodeca-2, 4, 6, 10-tetraenal) had lower binding energy values than others. Despite the low binding energy of the PEOC14 molecule, no hydrogen bond was produced when the complex link between protein and ligand was observed.

Therefore, the PEOC14 molecule was assumed to have less inhibitory activity on aging-causing proteins. PEOC27 and PEOC28 showed promising effectiveness against target proteins. The PEOC27 compound had a low binding energy value with MMP13 and hyaluronidase, while PEOC28 had a low binding energy value with MMP9. The number of hydrogen bond donors and acceptors indicates the compound's ability to interact with the target protein. The number of hydrogen bonds formed determines the strength of the interaction between the ligand and the target protein. Ligands that interact with the target protein through hydrogen bonding have higher bond stability than those that do not.[23]

The molecular docking results were visualized in 2D and 3D structures as shown in Figure 2. The figure on the left shows a 3D structure of the protein-ligand complex, while the figure on the right presents the ligand-protein bond in 2D. Each position of the ligand that binds to the protein appears to be favorable, as indicated by the position in the pocket on the protein surface. According to Deniz *et al*.,[32] the more highly polar the interactions between the ligand and protein, the better the interaction between the complex. The polar side of the protein is usually located in the pocket, hence, when a ligand enters the pocket, it is considered to have a good interaction with the protein. The hydrophobic surfaces, also known as ligand binding pockets, improve the flexibility and stability of protein-ligand complexes.[33] Meanwhile, the hydrophobic surface and polar bond work together to maintain protein thermodynamic stability. Ligands can activate bioactivity by binding to the hydrophobic areas of proteins.[34] Hydrophobic bonding is essential for protein structure, lipid transport through plasma proteins, and steroid receptor binding.

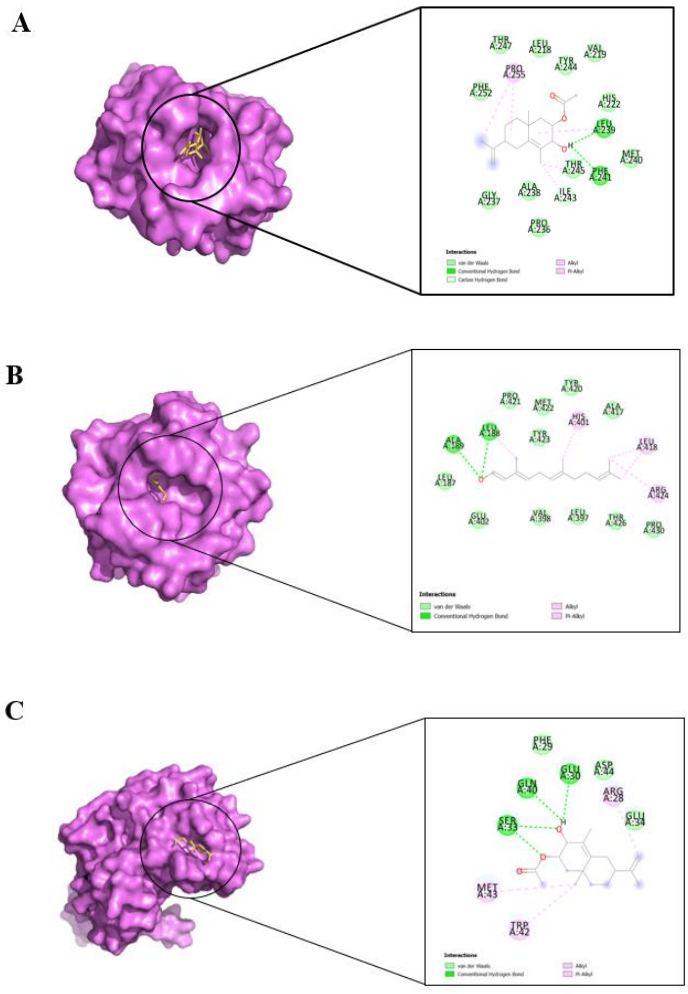

Figure 2: Visualization in 3D and 2D of molecular docking result. **(A)** MMP13 with Acetic acid, 3-Hydroxy-6-isopropenyl; **(B)** MMP9 with 3, 7, 11-Trimethyl-dodeca-2, 4, 6, 10-tetraenal; **(C)** Hyaluronidase with Acetic acid, 3-Hydroxy-6-isopropenyl.

Table 3: Predicted Toxicity of selected 26 PEO compounds

Compound	Toxicity				TC (Toxicity Class)	LD_{50}
	Carcinogenic	Immunotoxin	Mutagenic	Cytotoxic		
PEOC1	Active*	Inactive	Inactive	Inactive	5	3200 mg/kg
PEOC10	Inactive*	Active	Inactive	Inactive	5	5000mg/kg
PEOC11	Inactive*	Inactive	Inactive	Inactive*	4	2000 mg/kg
PEOC12	Inactive	Inactive	Inactive	Inactive	4	940 mg/kg
PEOC13	Inactive*	Inactive*	Inactive	Inactive	5	5000 mg/kg
PEOC14	Inactive*	Inactive	Inactive	Inactive	5	5000 mg/kg
PEOC15	Inactive	Inactive	Inactive	Inactive	5	5000 mg/kg
PEOC16	Active*	Inactive	Inactive*	Inactive	5	5000 mg/kg
PEOC22	Inactive	Inactive	Inactive	Inactive	5	5000 mg/kg
PEOC23	Inactive*	Active*	Inactive	Inactive	5	5000 mg/kg
PEOC24	Inactive*	Inactive*	Inactive	Inactive	5	3900 mg/kg
PEOC25	Inactive*	Inactive	Inactive	Inactive	4	2000 mg/kg
PEOC26	Inactive*	Inactive	Inactive	Inactive	5	3900 mg/kg
PEOC27	Active*	Inactive	Inactive	Inactive	5	3000 mg/kg
PEOC28	Inactive	Inactive	Inactive	Inactive	5	5000 mg/kg
PEOC29	Inactive*	Inactive	Inactive	Inactive	5	5000 mg/kg
PEOC35	Inactive*	Inactive	Inactive	Inactive	5	3000 mg/kg
PEOC36	Inactive	Inactive	Inactive	Inactive	5	5000 mg/kg
PEOC37	Inactive*	Active*	Inactive	Inactive	5	5000 mg/kg
PEOC38	Inactive*	Inactive	Inactive	Inactive	5	5000 mg/kg
PEOC39	Inactive	Inactive	Inactive	Inactive*	5	5000 mg/kg
PEOC40	Inactive*	Inactive	Inactive	Inactive	4	2000 mg/kg
PEOC41	Inactive	Inactive	Inactive	Inactive	4	5000 mg/kg
PEOC42	Inactive	Inactive	Inactive	Inactive	5	5000 mg/kg
PEOC43	Inactive*	Inactive	Inactive	Inactive	5	5000 mg/kg
PEOC44	Active*	Inactive	Inactive	Inactive	5	3000 mg/kg
RC1	Inactive	Inactive	Inactive	Inactive	5	2500 mg/kg
RC2	Inactive*	Inactive*	Active*	Inactive	4	1510 mg/kg
RC3	Inactive	Inactive	Inactive	Inactive	4	800 mg/kg

*Low probability (0-0,69)
Toxicity Class classifications: 1: fatal if swallowed (LD50 ≤ 5); Class 2: fatal if swallowed (5 < LD50 ≤ 50); Class 3: toxic if swallowed (50 < LD50 ≤ 300); Class 4: harmful if swallowed (300 < LD50 ≤ 2000); Class 5: may be harmful if swallowed (2000 < LD50 ≤ 5000); Class 6: non-toxic (LD50 > 5000) (GHS)

Based on the molecular docking result as presented in Figure 2, each of the interactions between proteins and ligands showed more than one hydrogen bond. The interaction between MMP13 and 3-Hydroxy-6-isopropenyl acetic acid had two hydrogen bonds at amino acid residues LEU239 and PHE241. The interaction between MMP9 and 3, 7, 11-Trimethyl-dodeca-2, 4, 6, 10-tetraenal had two hydrogen bonds at residues LEU188 and ALA189. Hyaluronidase with Acetic acid, 3-Hydroxy-6-isopropenyl interaction showed three hydrogen bonds at amino acid residues GLU30, SER33, and GLN40. The hydrogen bonds are shown on the amino acids that are slightly darker green in colour. This indicates that there is a good interaction between the ligand and the protein.

According to the 2D visualization results, the three main types of interactions that form between the ligand and protein complexes are hydrogen, hydrophobic, and van der Walls. These interactions provide the ligand with a substantial amount of stability. In addition, the number of hydrogen bonds formed influences the stability of the ligands. As previously stated, the number of hydrogen bonds formed during the protein-ligand interaction influences the stability of the complex structure.[35] In other words, the higher the number of hydrogen bonds formed, the stronger the contact between the protein complex and the ligand.

Molecular Dynamics Simulations Result

A molecular dynamics analysis was performed to predict the stability of the binding interactions between the ligand and the target protein. The results for each protein (MMP9, MMP13, and hyaluronidase) with each ligand are summarized in Table 5. All protein-ligand interactions had a favorable ligand RMSD value of less than 3 Å. Based on the RMSD ligand movement, Acetic acid and 3-Hydroxy-6-isopropenyl compounds that interacted with the MMP13 protein yielded a higher value compared to the hyaluronidase protein.

This significant result indicates that ligand molecules move at a specified period away from the active site of the protein.

The molecular dynamics simulation (MDS) result showed that the RMSD value of the ligand was lower compared to the equivalent control ligand (red line) (Figure 3). This indicates that each active compound has minimal movement compared to the control compound. According to Ali (2020),[36] the RMSD value can be used to calculate the magnitude of ligand shape or orientation changes after binding to the protein. This can help in the search for new drugs since ligands that bind to target proteins with low RMSD values are more likely to be promising candidates. The compounds do not need to significantly change shape to interact with proteins and work directly in metabolic pathways.[37]

As previously mentioned, the better ligand RMSD value is the lowest since it corresponds to a stronger connection. Based on the MDS result, the ligands 3, 7, 11-trimethyl-dodeca-2, 4, 6,10-tetraenal, and Acetic acid 3-hydroxy-6-isopropenyl can be considered potential drug candidates due to the low RMSD values. RMSD ligand movement is another MDS consequence. It demonstrates the ligand's stability when in contact with the protein. Low RMSD ligand movement usually implies a closer interaction with the target, which promotes ligand binding. When the ligand does not move considerably during the simulation (a low ligand movement RMSD value), it is considered stable.[38]

The result of RMSD ligand movement shows that Acetic Acid, and 3-hydroxy-6-isopropenyl move more rapidly in MMP13 protein (b) than the control compound (retinol) (Figure 4). In comparison to the other two proteins, Acetic acid 3-hydroxy-6-isopropenyl is less active at inhibiting MMP13. To support the efficacy as a potential treatment for skin aging, the other two proteins, MMP9 and hyaluronidase, demonstrated lower ligand mobility compared to the control. This also indicates a good interaction between the compound and the protein, making the compound a potential drug candidate.

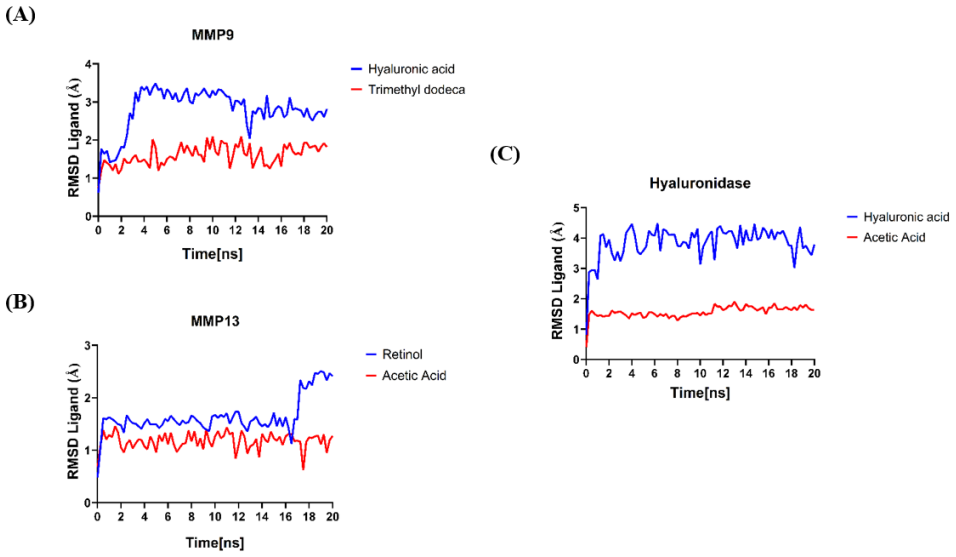

Figure 3: Graph Showing RMSD of PEO ligand (red line) against control ligand (blue line). **(A)** MMP9 protein; **(B)** MMP13 protein; **(C)** Hyaluronidase enzyme.

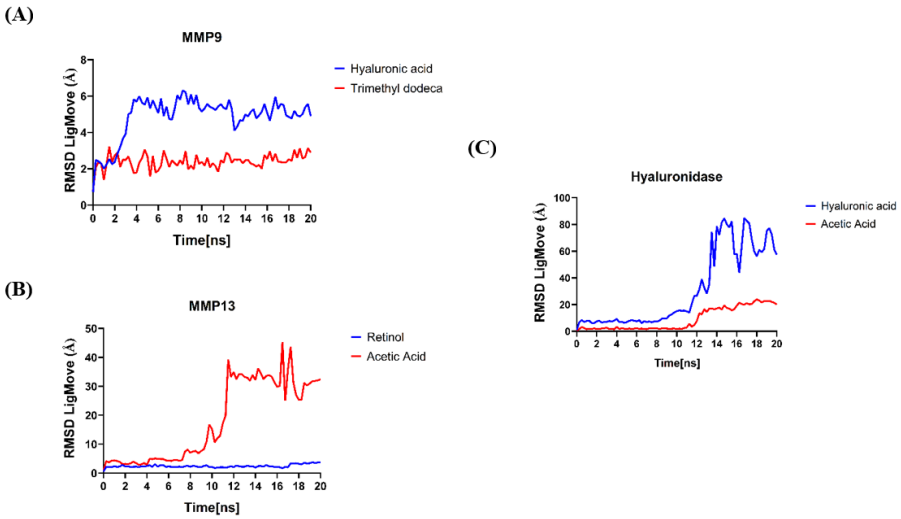

Figure 4. Graph showing RMSD of ligand movement of PEO Compound (red line) against control ligand (blue line). (a) MMP9 protein; (b) MMP13 protein; (c) Hyaluronidase enzyme.

Table 4: Molecular docking result between PEO ligands and reference compounds (RC) against target proteins with the lowest binding energy values

Compound	Binding Energy (Kcal/mol)		
	MMP13	**MMP9**	**Hyaluronidase**
RC1	-3,9	-6.0	-2.3
RC2	**-8.4**	-7.4	-6.4*
RC3	-6.0	**-7.9**	**-5.7**
PEOC13	-7.3	-7.8	-6.4
PEOC14	-7.6*	-6.3	-6.4
PEOC27	**-7.9**	-6.9	**-6.8**
PEOC28	-7.6	**-8.2**	-5.6

*The binding energy value is low, but there is no hydrogen bond between the ligand and the protein. The bolded result is the selected result.

Table 5: Molecular Dynamics Simulations result of each protein with ligand interacted

No.	MDS Parameters	Trimethyl Dodeca-MMP9	Acetic Acid-MMP13	Acetic Acid-Hyaluronidase
1	RMSD Ligand	1.603 Å	1.177 Å	1.566 Å
2	RMSD Ligand Movement	2.397 Å	17.821 Å	8.924 Å
3	RMSD Backbone	2.603 Å	1.709 Å	1.150 Å
4	Binding Energy	27.350 KJ/mol	-15.075 KJ/mol	-21.780 KJ/mol
5	No. of H Bond	285.215 Å	300.778 Å	552.728 Å
6	RMSF	PHE110, GLU111, GLY112, ASP113	PHE175, TYR176, PRO181, GLY 180	LEU333, ASN68, PRO67, ARG259

Aside from the previously mentioned parameters, the MDS analysis result includes the binding energy value and backbone RMSD. The binding energy value represents the strength of the interaction between the ligand and the protein over a given time. This value is determined using the MMPBSA method.[39] The calculation of the binding free energy value of MMPBSA in kJ/mol was performed by applying the addition principle. This principle requires the combination of various energy modules, including covalent, columbic, solvation of ligand and protein hydrogen bonds, van der Waals, and lipophilic interactions. In contrast to molecular docking, MMPBSA analysis of the complexes led to an increase in binding energy values, indicating the capacity of the compounds to interact efficiently with the respective proteins. The value obtained was different compared to the molecular docking result.[39] The result showed that the binding energy value between the 3, 7, 11-trimethyl-dodeca-2, 4, 6,10-tetraenal ligand molecule and the MMP9 protein was higher than the other two proteins. A positive binding energy value, according to the MMPBSA calculation, is an appropriate criterion for characterizing the binding interaction between the ligand molecule and the target protein (Figure 5).

Backbone RMSD values provide details about changes in a protein shape or conformation upon binding to a ligand. Table 5 shows that the average backbone RMSD value for each protein is less than 3 Å. When evaluated graphically (Figure 6), the conformational changes shown by each protein indicate a pattern of movement quite similar to that observed when the protein binds to the control compound. Similar movement of protein conformational changes between the studied compound and the control indicates great potential as an alternative candidate.[41] The MMP9 protein activity increased significantly during interaction with the 3, 7, 11-trimethyl-dodeca-2, 4, 6,10-tetraenal molecule. However, this does not indicate that the ligand separated or moved away from the active side of the protein during the simulation. The ligand continues to interact with the protein through hydrophobic interactions until the end of the simulation. The interactions are stabilized by hydrophobic and hydrogen bonds.[42,43]

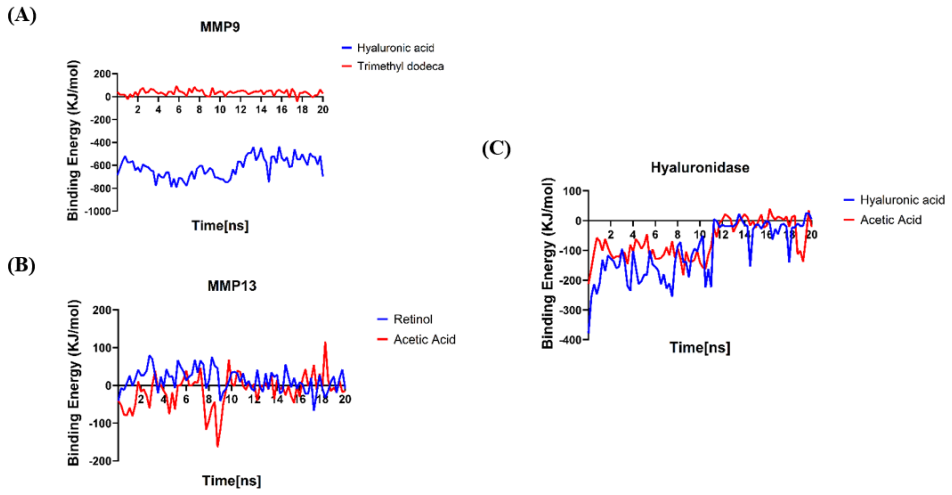

Figure 5: Graph showing the Binding Energy of each PEO ligand (red line) against the control ligand (blue line). **(A)** MMP9 protein; **(B)** MMP13 protein; **(C)** Hyaluronidase enzyme

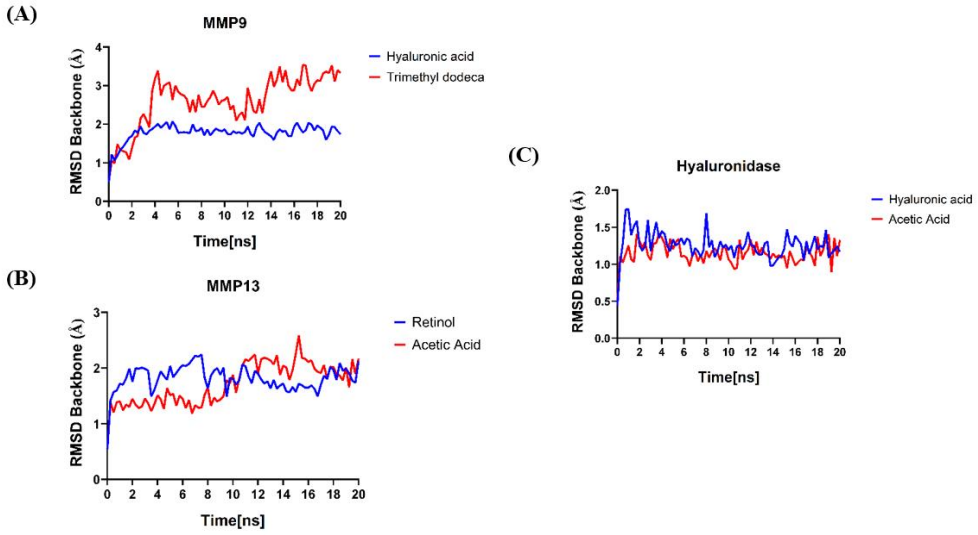

Figure 6: Graph showing RMSD Backbone of each PEO Compound (red line) against the control ligand (blue line). **(A)** MMP9 protein; **(B)** MMP13 protein; **(C)** Hyaluronidase enzyme

Conclusion

In conclusion, PEO active compounds have the potential to function as inhibitors of proteins associated with skin aging. The compounds 3,7,11-trimethyl-dodeca-2,4,6,10-tetraenal and 3-hydroxy-6-isopropenyl acetic acid demonstrated effective inhibitory activity compared to the control. Furthermore, MDS results showed that both compounds have high binding stability with the proteins that cause skin aging, namely, MMP13, MMP9, and hyaluronidase. This suggests that efficacious drug products can be developed using the PEO-active compounds. It is also expected that through this research, an anti-aging therapeutic product can be developed.

Conflicts of interest

The authors declare no conflicts of interest.

Authors' Declaration

The authors hereby declare that the work presented in this article are original and that any liability for claims relating to the content of this article will be borne by them.

Acknowledgments

The authors are grateful to the Master Program, Biology Department, and Laboratory of Genetics and Molecular Biology, Faculty of Mathematics and Natural Sciences, Syiah Kuala University, for facilitating the study. This study was supported by the Technology and Community Service (DRTPM), the Institute of Research and Community Services (LPPM), Universitas Syiah Kuala, under a Master Thesis Grant with contract number 168/E5/PG.02.00.PL/2023.

References

1. Dar RA, Shahnawaz M, Rasool S, Qazi PH, Qazi H. Natural product medicines: A literature update. J Phytopharm. 2017; 6(6):340–342.
2. Xie T, Ding Q, Feng S, Liu Z, Shi Y. Antioxidant mechanism of modified Qiongyu paste against aging based on network

pharmacology and experimental validation. J Tradit Chinese Med Sci. 2022; 9(4):420–431.
3. van Beek TA and Joulain D. The essential oil of patchouli, *Pogostemon cablin*: A review. Flavour Fragr J. 2018; 33(1):6–51.
4. Rahmi D, Yunilawati R, Jati BN, Setiawati I, Riyanto A, Batubara I, Astuti IR. Indonesian Essential Oils. Cosmetics. 2021;8(4):1–9.
5. Ganceviciene R, Liakou AI, Theodoridis A, Makrantonaki E, Zouboulis CC. Skin anti-aging strategies. Dermatoendocrinol. 2012;4(3):308–319.
6. Jacczak B, Rubiś B, Totoń E. Potential of naturally derived compounds in telomerase and telomere modulation in skin senescence and aging. Int J Mol Sci. 2021;22(12):1–22.
7. Nafissa N, Isnaini N, Desiyana LS, Prajaputra V, Harnelly E, Zulkarnain Z, Maryam S. Patchouli and Essential Oil Products Antiaging Mechanism of Natural Plant Sources: A Potential Current Product. J Patchouli Essent Oil Prod. 2023; 2(2):41–47.
8. Pittayapruek P, Meephansan J, Prapapan O, Komine M, Ohtsuki M. Role of Matrix Metalloproteinases in Photoaging and Photocarcinogenesis. Int J Mol Sci. 2016; 17(6):1–20.
9. Younis MM, Ayoub IM, Mostafa NM, El Hassab MA, Eldehna WM, Al-Rashood ST, Eldahshan OA. GC/MS Profiling, Anti-Collagenase, Anti-Elastase, Anti-Tyrosinase and Anti-Hyaluronidase Activities of a *Stenocarpus sinuatus* Leaves Extract. Plants. 2022; 11(7):918.
10. Jakimiuk K, Sari S, Milewski R, Supuran CT, Şöhretoğlu D, Tomczyk M. Flavonoids as tyrosinase inhibitors *in silico* and *in vitro* models: basic framework of SAR using a statistical modelling approach. J Enzyme Inhib Med Chem. 2022; 37(1):427–436.
11. Eun Lee K, Bharadwaj S, Yadava U, Gu Kang S. Evaluation of caffeine as inhibitor against collagenase, elastase and tyrosinase using *in silico* and *in vitro* approach. J Enzyme Inhib Med Chem. 2019; 34(1):927–936.
12. Kongsompong S, E-kobon T, Taengphan W, Sangkhawasi M, Khongkow M, Chumnanpuen P. Computer-Aided Virtual Screening and In Vitro Validation of Biomimetic Tyrosinase Inhibitory Peptides from Abalone Peptidome. Int J Mol Sci. 2023; 24(4):3154.
13. Sinha S, Biswas D, Mukherjee A. Antigenotoxic and antioxidant activities of palmarosa and citronella essential oils. J Ethnopharmacol. 2011; 137(3):1521–1527.
14. Baig MH, Ahmad K, Adil M, Khan ZA, Khan MI, Lohani M, Khan MS, Kamal MA. Drug Discovery and *In Silico* Techniques: A Mini-Review. Enzym Eng. 2014; 03(02):1–3.
15. Annisa A. Antidepressant Activity Test of Patchouli Oil Light Fraction (*Pogostemon cablin*) Against Rats (*Rattus novergicus*) with Tail Suspension Test Method. Syiah Kuala University; 2024.
16. Isnaini N, Khairan K, Faradhilla M, Sufriadi E, Prajaputra V, Ginting B, Muhammad S, Rufika RD. A Study of Essential Oils from Patchouli (*Pogostemon cablin* Benth.) and Its Potential as an Antivirus Agent to Relieve Symptoms of COVID-19. J Patchouli Essent Oil Prod. 2022; 1(2):27–35.
17. Syaharani CPS, Isnaini N, Harnelly E, Prajaputra V, Maryam S, Gani FA. A Systematic Review: Formulation of Facial Wash Containing Essential Oil. J Patchouli Essent Oil Prod. 2023; 2(1):9–15.
18. Mathey P, Lirette F, Fernández I, Renn L, Weitz RT, Morin JF. Annulated Azuleno [2,1,8-ija] azulenes Synthesis and Properties. Angew Chemie Int Ed. 2023; 62:e202216281.
19. Widyasanti A, Nurjanah S, Nurhadi B, Osman CP. Optimization of the Vacuum Fractional Distillation Process for Enhancing the α-Guaiene of Patchouli Oil with Response Surface Methodology. Separations. 2023; 10(9):469–487.
20. Iskandar B, Tartilla R, Lukman A, Leny L, Surboyo MDC. Anti-aging Activity Test of Patchouli Oil Microemulsion (*Pogostemon cablin* Benth.). Maj Farmasetika. 2022; 7(1):52.
21. Wu J, Pan L. Study on the Effect of *Pogostemon Cablin* Benth on Skin Aging Based on Network Pharmacology. Curr Comput Aided Drug Des. 2022; 18(6):459–468.
22. Taufik M, Rizal S, Harnelly E, Muhammad S, Syahrizal D, Prajaputra V, Isnaini N. The Therapeutic Potential of Aceh Patchouli Oil (*Pogostemon cablin* Benth.) in Enhancing Full-Thickness Wound Healing in Mice. Trop J Nat Prod Res. 2024; 8(1):5840–5844.
23. Nur S, Hanafi M, Setiawan H, Nursamsiar, Elya B. In silico evaluation of the dermal antiaging activity of *Molineria latifolia* (Dryand. ex W.T. Aiton) Herb. Ex Kurz compounds. Trop J Nat Prod Res. 2023;11(2):325–345.
24. Daina A, Michielin O, Zoete V. SwissADME: A free web tool to evaluate pharmacokinetics, drug-likeness and medicinal chemistry friendliness of small molecules. Sci Rep. 2017; 7(10):1–13.
25. Shi J, Wang J, Jia N, Sun Q. A network pharmacology study on mechanism of resveratrol in treating preeclampsia via regulation of AGE-RAGE and HIF-1 signalling pathways. Front Endocrinol (Lausanne). 2023; 13(1):1–12.
26. Dumont C, Prieto P, Asturiol D, Worth A. Review of the Availability of *In Vitro* and *In Silico* Methods for Assessing Dermal Bioavailability. Appl Vitr Toxicol. 2015; 1(2):147–164.
27. Ismail NZ, Khairuddean M, Alidmat MM, Abubakar S, Arsad H. Cytotoxicity effect, network pharmacology, molecular docking, and molecular dynamics simulation of new mono-chalcone compounds for breast cancer. Res Sq. 2023; 1–40.
28. Gobbi A, Herman K, Bizzoco L, Avio G. Evaluation of Safety and Performance of Hyaluronic Acid Combined with Niacinamide Versus Standard Infiltrative Therapy in the Treatment of Joint Degenerative and Post-Traumatic Diseases. J Orthop Muscular Syst. 2023; 6(2):1–6.
29. Zerbinati N, Lotti T, Monticelli D, Martina V, Cipolla G, D'Este E, Calligaro A, Mocchi R, Maccario C, Sommatis S, Lotti J, Wollina U, Tchernev G, França K. *In vitro* evaluation of the sensitivity of a hyaluronic acid PEG cross-linked to bovine testes hyaluronidase. Maced J Med Sci. 2018; 6(1):20–24.
30. Banerjee P, Eckert AO, Schrey AK, Preissner R. ProTox-II: A webserver for the prediction of toxicity of chemicals. Nucleic Acids Res. 2018; 46(W1):257–263.
31. Lu Z, Gao F, Teng F, Tian X, Guan H, Li J, Wang X, Liang J, Tian Q, Wang J. Exploring the pathogenesis of depression and potential antidepressants through the integration of reverse network pharmacology, molecular docking, and molecular dynamics. Medicine (Baltimore). 2023; 102(44):e35793.
32. Deniz FSS, Salmas RE, Emerce E, Cankaya IIT, Yusufoglu HS, Orhan IE. Evaluation of collagenase, elastase and tyrosinase inhibitory activities of *Cotinus coggygria* Scop. through *in vitro* and *in silico* approaches. South African J Bot. 2020; 132:277–288.
33. Lee S and Barron MG. Structure-Based Understanding of Binding Affinity and Mode of Estrogen Receptor α Agonists and Antagonists. PLoS One. 2017; 12(1):e0169607.
34. Ferenczy GG and Kellermayer M. Contribution of hydrophobic interactions to protein mechanical stability. Comput Struct Biotechnol J. 2022; 20(1):1946–1956.
35. Bitencourt-Ferreira G and de Azevedo WF. Docking Screens for Drug Discovery. Vol. 2053, Methods in Molecular Biology. 2019. 189–202 p.
36. Ali MA. Molecular docking and molecular dynamics simulation of anticancer active ligand '3,5,7,3′,5′-pentahydroxy-flavanonol-3-O-α-L-rhamnopyranoside' from *Bauhinia strychnifolia* Craib to the cyclin-dependent protein kinase. J King Saud Univ - Sci. 2020; 32(1):891–895.
37. Singh S, Bani Baker Q, Singh DB. Molecular docking and molecular dynamics simulation. In: Bioinformatics: Methods and Applications. 2021. 291–304 p.
38. Martínez L. Automatic identification of mobile and rigid substructures in molecular dynamics simulations and fractional structural fluctuation analysis. PLoS One. 2015;

10(3):1–10.
39. Luthfiana D and Utomo DH. Network pharmacology reveals the potential of Dolastatin 16 as a diabetic wound healing agent. Silico Pharmacol. 2023; 11(1):1–25.
40. Sharma J, Bhardwaj VK, Singh R, Rajendran V, Purohit R, Kumar S. An *in-silico* evaluation of different bioactive molecules of tea for their inhibition potency against non structural protein-15 of SARS-CoV-2. Food Chem. 2021; 346:1–8.
41. Stanzione F, Giangreco I, Cole JC. Use of molecular docking computational tools in drug discovery. 1st ed. Vol. 60, Progress in Medicinal Chemistry. Elsevier B.V.; 2021. 273–343 p.
42. Utomo DH and Kita M. Binding Mode of Actin–Aplyronine A–Tubulin Heterotrimeric Complex Revealed by Molecular Dynamics Simulation. Bull Chem Soc Jpn. 2023; 96(2):120–126.
43. Syahraini A, Harnelly E, Hermanto FE. Pro-Apoptosis Activity of *Pogostemon cablin* Benth. Against Nasopharyngeal Carcinoma through the BCL-2 Inhibition Signaling Pathway: A Computational Investigation. Makara J Sci. 2023; 27(3):208–216.